Identification of a native low-conductance NMDA channel with reduced sensitivity to Mg^{2+} in rat central neurones

Akiko Momiyama, Dirk Feldmeyer and Stuart G. Cull-Candy *

Department of Pharmacology, University College London, Gower Street, London WC1E 6BT, UK

1. We have identified a new type of NMDA channel in rat central neurones that express mRNA for the NR2D subunit. We have examined single NMDA channels in cerebellar Purkinje cells (which possess NR1 and 2D), deep cerebellar nuclei (NR1, 2A, 2B and 2D) and spinal cord dorsal horn neurones (NR1, 2B and 2D).

2. In Purkinje cells, NMDA opened channels with a main conductance of 37·9 ± 1·1 pS and a subconductance of 17·8 ± 0·7 pS, with frequent transitions between the two levels.

3. NMDA activated low-conductance ('38/18 pS') events (along with high-conductance – '50/40 pS' – openings) in some patches from deep cerebellar nuclei and dorsal horn neurones. Our evidence suggests that 38/18 pS and 50/40 pS events arose from distinct types of NMDA receptors.

4. The transitions for 38/18 pS events were asymmetrical: steps from 38 to 18 pS were more frequent (72·2%) than steps from 18 to 38 pS. This feature appeared common to the 38/18 pS events in all three cell types, suggesting similarity in the low-conductance channels.

5. The 38/18 pS channels in Purkinje cells exhibited characteristic NMDA receptor properties, including requirement for glycine, antagonism by D-2-amino-5-phosphonopentanoic acid (D-AP5) and 7-chlorokynurenic acid, and voltage-dependent block by extracellular Mg^{2+}.

6. The mean open time for the 38 pS state (0·74 ± 0·07 ms) was significantly briefer than that for the 18 pS state (1·27 ± 0·18 ms).

7. Mg^{2+} block of low-conductance NMDA channels in Purkinje cells was less marked than block of 50/40 pS channels in cerebellar granule cells.

8. The time course of appearance of 38/18 pS NMDA channels matched the expression of mRNA for the NR2D subunit. Thus 38/18 pS events were present in >70% of Purkinje cell patches in 0- to 8-day-old animals, and absent by postnatal day 12.

9. We propose that the 38/18 pS NMDA channels identified here (associated with the NR2D subunit), and the other low-conductance NMDA channel associated with the NR2C subunit, may together constitute a functionally distinct subclass of *native* NMDA receptors.

N-methyl-D-aspartate (NMDA) receptors appear to be unique among mammalian synaptic receptors in possessing a number of distinctive features including voltage-dependent block by Mg^{2+} ions, permeability to Ca^{2+} ions, high sensitivity to H^+ at physiological pH, slowly decaying currents and a requirement for binding of the co-agonist glycine for their activation. This complex combination of features appears to confer on NMDA receptors an ability to promote various forms of synaptic plasticity in the CNS, including developmental and synaptic changes. Recent evidence, provided by molecular cloning (reviewed by McBain & Mayer, 1994), has revealed several cDNA species encoding distinct NMDA receptor subunits. This raises the possibility that these critical NMDA receptor features may vary throughout the CNS.

Molecular cloning studies have identified a family of NMDA receptor subunits – namely, the ubiquitously expressed NR1 subunit and four NR2 subunits: NR2A, NR2B, NR2C and NR2D (see Moriyoshi, Masu, Ishii, Shigemoto, Mizuno & Nakanishi, 1991; Ikeda *et al.* 1992; Kutsuwada *et al.* 1992; Meguro *et al.* 1992; Yamazaki, Mori, Araki, Mori & Mishina, 1992; Hollmann *et al.* 1993; Ishii *et al.* 1993;

* To whom correspondence should be addressed.

Monyer, Burnashev, Laurie, Sakmann & Seeburg, 1994; reviewed by McBain & Mayer, 1994). Each of the NR2 subunits forms functional recombinant receptors with the NR1 subunit, to give channels with characteristic properties (see Monyer *et al.* 1992, 1994). This, together with the distinct temporal and spatial expression of mRNAs for different NR2 subunits (Ikeda *et al.* 1992; Kutsuwada *et al.* 1992; Ishii *et al.* 1993; Akazawa, Shigemoto, Bessho, Nakanishi & Mizuno, 1994; Monyer *et al.* 1994; Watanabe, Mishina & Inoue, 1994*a*, *b*), further supports the idea of functionally diverse types of NMDA receptors. This could have important consequences, as the properties of NMDA receptors will influence the role they play in cell signalling.

Surprisingly, while binding measurements support the presence of several distinct populations of NMDA receptors *in situ*, only a few functional studies have found evidence for biophysical or pharmacological variation among *native* NMDA receptors. Thus, developmental changes that may be attributable to alteration in subunit composition have been described in the kinetics of the NMDA component of excitatory postsynaptic currents (EPSCs) in the visual cortex (Carmignoto & Vicini, 1992) and superior colliculus (Hestrin, 1992), and in the kinetics and conductance of NMDA channels in the cerebellum (Cull-Candy, Howe & Usowicz, 1987; Farrant, Feldmeyer, Takahashi & Cull-Candy, 1994; Feldmeyer, Farrant & Cull-Candy, 1995). In recent single-channel studies, the unique single-channel properties of NMDA receptors in mature granule cells correlates well with the expression of the NR2C subunit (Farrant *et al.* 1994). Furthermore, these native channels exhibit features which match those of the recombinant NR2C-containing NMDA receptors (Stern, Béhé, Schoepfer & Colquhoun, 1992). However, the potentially powerful approach of identifying native NMDA receptors on the basis of their single-channel properties has not yet been employed for the more widespread receptors associated with other NR2 subunit species.

mRNA for the NR2D subunit is widespread in the CNS, particularly in embryonic and neonatal animals (peaking at around 7 days after birth; see Monyer *et al.* 1994), consistent with the idea that this subunit could contribute to receptors involved in developmental processes. Furthermore, some types of neurones show significant expression of NR2D mRNA in the adult. These include dorsal and ventral horn neurones in the spinal cord, some interneurones in the hippocampus, stellate/basket cells of the cerebellum and neurones of the deep cerebellar nuclei (Ishii *et al.* 1993; Tölle, Berthele, Zieglgänsberger, Seeburg & Wisden, 1993; Akazawa *et al.* 1994; Monyer *et al.* 1994). This subunit is of particular interest as the recombinant NR1/NR2D receptors are known to exhibit an unusually low sensitivity to block by extracellular Mg^{2+} ions (Monyer *et al.* 1994). Voltage-dependent block of NMDA receptors by Mg^{2+} allows them to function as activity sensors, permitting Ca^{2+} and Na^{+} influx through channels only in those cells that receive high-frequency synaptic inputs.

We have examined Purkinje cells, which in the early postnatal period (postnatal days 0–8) express mRNAs for only NR1 and NR2D (Akazawa *et al.* 1994). The evidence for functional NMDA receptors in Purkinje cells has previously been equivocal. We have also studied spinal cord dorsal horn neurones and deep cerebellar nuclei neurones that express mRNAs for other NR2 subunits along with NR2D (see Monyer *et al.* 1994; Akazawa *et al.* 1994). Our experiments indicate the existence of a distinct type of low-conductance NMDA channel in patches from these neurones that express mRNA for the 2D subunit. The channels can be readily identified from their characteristic channel conductances, and other properties that appear distinct from the 50 pS type of NMDA channel.

A preliminary report of some of these results appeared in this journal (Momiyama, Feldmeyer & Cull-Candy, 1995).

METHODS

Preparation and recording

Parasagittal slices (150–200 μm) from cerebella of 1- to 12-day-old Sprague–Dawley rats were prepared as described previously (Farrant & Cull-Candy, 1991; Farrant *et al.* 1994). Animals were decapitated and cerebella were sliced with a vibrating microslicer (DTK-1000, Dosaka Co. Ltd, Kyoto, Japan) in cold (2–4 °C) oxygenated Krebs solution. Before recording, slices were incubated for 1 h at 32 °C. Subsequently, slices were maintained at room temperature (20–25 °C) and used for recording for up to 8 h after preparation. For experiments, slices were transferred into a recording chamber that was positioned under an upright microscope (Axioscope; Zeiss, Oberkochen, Germany) and viewed under Nomarski optics (total magnification, ×640–1024). Purkinje cells were identified by their location at the boundary between the internal granular and molecular layer, and by their large soma diameter and characteristic morphology when filled with the fluorescent dye Lucifer Yellow (0·3% in pipette solution). We found an age-dependent increase in the membrane capacitance of Purkinje cells (as measured with the patch-clamp amplifier; P1, 16·2 ± 1·6 pF, $n = 8$; P2, 20·3 ± 2·2 pF, $n = 13$; P4, 25·7 ± 3·6 pF; $n = 6$; P5, 36·0 ± 2·6 pF; $n = 32$). Neurones of the deep cerebellar nuclei were visually identified from their location in the white matter. Transverse slices of lumbar spinal cord (150–180 μm thick) were prepared from 2- to 5-day-old Sprague–Dawley rats. The spinal cord was taken out in cold oxygenated Krebs solution, following decapitation. Dural and pial membranes were removed and the tissue was immersed in Krebs solution containing 4% agar (35 °C). This was cooled (to harden the agar) and cut into a small block containing the lumbar part of the spinal cord. The tissue-containing agar block was sliced and incubated. For patch-clamp experiments dorsal horn neurones were identified visually.

Patch pipettes were pulled from thick-walled glass tubing (GC150F-7.5; Clark Electromedical), coated with Sylgard resin (Dow Corning 184) and fire polished to a final resistance of 5–10 MΩ for recordings in the whole-cell mode or 10–15 MΩ for outside-out patches. Recordings were made at room temperature using either an Axopatch-1D or an Axopatch 200A patch-clamp amplifier (Axon Instruments) and stored on FM tape (Racal Store 4; DC to 5 kHz) or on digital audio tape (BioLogic DTR-1204; DC to 20 kHz) for further analysis.

Solutions

The composition of the incubating Krebs solution was as follows (mM): NaCl, 125; KCl, 2·5; $CaCl_2$, 1; $MgCl_2$, 5; $NaHCO_3$, 26; NaH_2PO_4, 1·25; glucose, 15; lactate, 4. The recording solution was essentially of the same composition but without $MgCl_2$ and lactate. Potentiometric measurements of ionized Ca^{2+} with a Ca^{2+}-sensitive electrode (Orion Research Inc., Boston, MA, USA) yielded a free Ca^{2+} concentration of 0·84 ± 0·01 mM ($n = 3$, bubbled with 95% O_2 and 5% CO_2; pH 7·4). Drugs were added to the perfusate. Bicuculline methiodide, 6-cyano-7-nitroquinoxaline-2,3-dione (CNQX), D-2-amino-5-phosponopentanoic acid (D-AP5), 7-chloro-kynurenate and NMDA were obtained from Tocris Cookson (Bristol, UK) and L-glutamate, glycine, strychnine and tetrodotoxin (TTX) from Sigma. All experiments were carried out in the presence of 10 μM bicuculline, 10 μM CNQX and 500 nM strychnine; whole-cell NMDA currents were recorded in the presence of 300 nM TTX.

The pipette (intracellular) solution contained (mM): CsCl, 140; NaCl, 4; $CaCl_2$, 0·5 or 0·1; Hepes, 10; EGTA, 5 (adjusted to pH 7·3 with CsOH); occasionally 2 mM Mg-ATP was added. In some experiments, a CsF-containing internal solution of the following composition was used (mM): CsF, 110; CsCl, 30; NaCl, 4; $CaCl_2$, 0·5 or 0·1; Hepes, 10; EGTA, 5 (adjusted to pH 7·3 with CsOH). No difference was observed between recordings obtained with either pipette solution.

Single-channel analysis

Records were filtered with a continuously variable 8-pole Bessel filter to a final cut-off frequency of 2 kHz (−3 dB) and digitized at 20 kHz (Intel 80386-based personal computer equipped with a CED 1401+ interface or TL-1 DMA interface; Axon Instruments). Amplitudes and durations of single-channel events were determined by the method of time-course fitting (SCAN & EKDIST; Colquhoun & Sigworth, 1995). Mean current levels were determined from maximum likelihood fits of the mixture of two Gaussian distributions to the cursor-fitted amplitudes. Only openings longer than two filter rise times (332 μs) were included in the amplitude distributions. Chord conductances were calculated either by assuming a reversal potential of −3 mV (for Purkinje cell patches) or by using measured reversal potentials in individual patches. To determine the slope conductance, all-point amplitude histograms of single-channel recordings at several different membrane potentials were constructed using pCLAMP software (pCLAMP 6.0.1, Fetchan; Axon Instruments). The extrapolated reversal potential in Purkinje cell patches was −3·2 ± 0·6 mV ($n = 7$). No correction for liquid junction potential was made.

Before fitting open time distributions a resolution of 332 μs for channel openings was imposed. To compare the mean apparent open times of main and subconductance level, we used a closed time resolution which gave a false event rate of less than 10^{-6} s^{-1} for openings to the subconductance level (see Colquhoun & Sigworth, 1995); this was between 170 and 240 μs. The same closed time resolution was then used for openings to the main conductance level in order to exclude the effects of time resolution on the apparent open time distribution. The effect of Mg^{2+} on channel open time was studied only for openings to the more frequently occurring main conductance level using a resolution of two filter rise times (332 μs) for channel openings and 80–100 μs for channel closures. Open time distributions were fitted with single exponential functions by the maximum likelihood method. Open times were binned logarithmically and a square root transformation of the ordinate (events/bin) was used for display purposes. Plotted in this manner, the peak in the histogram corresponded to the time constant of the exponential component.

In the measurement of the frequency of direct transitions, conductance ranges were visually determined from the corresponding amplitude histogram. A resolution of 332 μs was used. Superimposing a different resolution did not affect our measured frequency of direct transitions. Occurrence of transitions between two states (represented as the ith conductance level followed by the $(i + 1)$th conductance level, where i is an integer) was shown as a single dot in displaying the frequency of various transition types (Kourie, Laver, Junankar, Gage & Dulhunty, 1996).

In order to quantify the blocking effect of AP5 or extracellular Mg^{2+}, charge transfer by single-NMDA channel currents was measured in the absence and presence of the blocker. This was necessary because the NMDA current density in Purkinje cells was too low to allow an accurate measurement of the amplitude of the whole-cell current.

RESULTS

Low-conductance NMDA channels in various central neurones

NMDA (10–50 μM) was applied to outside-out patches obtained from various neurone types that have previously been shown to express mRNA for the NR2D NMDA receptor subunit, either with NR1 alone or together with other NR2 subunits (Akazawa *et al.* 1994; Monyer *et al.* 1994). We have used thin slice preparations to examine Purkinje cells (postnatal 1- to 12-day-old animals: P1–12), deep cerebellar nuclei neurones (P4) and dorsal horn neurones of the spinal cord (P2–5). As illustrated in Fig. 1*A*, Purkinje cell patches gave single-channel openings to two conductance levels of 37·2 ± 0·6 and 17·6 ± 0·6 pS (chord conductances, $n = 15$) in nominally Mg^{2+}-free external solution. There were frequent direct transitions between the two conductance levels (5·2 ± 0·7%, $n = 13$), and the relative proportions of openings to these two levels were similar in all Purkinje cell patches studied (see later), as would be expected if they are different conductance states of the same channel. Openings to the 50 pS conductance level were not detected in any of the Purkinje cell patches ($n = 128$); thus all Purkinje cell patches that responded to NMDA exhibited only the 'low-conductance' type openings. For convenience we will usually refer to these events as '38/18 pS' openings (based on their slope conductance values in Purkinje cell patches) and the high-conductance events as '50/40 pS' openings, throughout the rest of this paper. As shown in Fig. 1*B* and *C*, NMDA activated low-conductance openings, along with 50/40 pS events, in approximately 80% of patches from deep cerebellar nuclei neurones, and in approximately 50% of patches from spinal cord neurones (these are denoted as 'mixed-type' patches in Fig. 1*B* and *C*). Other patches from these cells exhibited 50/40 pS openings in isolation (denoted 'high-conductance' patches in Fig. 1*B* and *C*).

Several pieces of evidence indicated that the low-conductance events in deep cerebellar nuclei neurones and spinal cord neurones arose from channels that were separate from the 50/40 pS NMDA-receptor channels, and resembled the low-conductance channels in Purkinje cells. Firstly, the

amplitude of the low-conductance levels in deep cerebellar nuclei neurones (37·9 ± 1·6 and 17·3 ± 1·0 pS, $n = 4$) and spinal cord neurones (38·3 ± 1·0 and 17·2 ± 0·3 pS, $n = 5$) were not significantly different from those in Purkinje cell patches ($P > 0·05$, Student's t test). Secondly, some patches from these neurones showed only 50/40 pS openings (Fig. 1*B* and *C*), indicating that these can occur independently of low-conductance openings.

Our analysis of the structure of transitions between different conductance levels provided further evidence that low-conductance 38/18 pS events arose from a separate receptor in the mixed-type patches. This is illustrated in Fig. 2. The graphs in the top panels give an indication of the frequency of occurrence of the various types of transition (each represented by a single dot) between any two possible states (i.e. above the dashed line: C (closed) → 18 pS (level 1), C → 38/40 pS (level 2), C → 50 pS (level 3), 18 → 38/40 pS, 38/40 → 50 pS; below the dashed line: 50 pS → C, 38/40 pS → C, 18 pS → C, 50 → 38/40 pS; 38/40 → 18 pS) in patches from Purkinje cells, deep cerebellar nuclei neurones and dorsal horn neurones. The histograms below each graph show the conductance levels present, and their relative proportions, in patches from the three cell types.

Two features were of particular interest in analysis of the sort shown in Fig. 2. While two types of open–open transitions were observed in Purkinje cell patches (Fig. 2*A*: graph and histogram) the prevalence of steps from 38 to 18 pS (2 → 1) greatly exceeded that of steps from 18 to 38 pS (1 → 2); thus 72·8% events were steps from 38 to 18 pS. Such asymmetry was observed in all Purkinje cell patches examined; 72·2% (data pooled from 13 patches) of transitions were steps from 38 to 18 pS (see also Cull-Candy & Usowicz, 1987). As is apparent from Fig. 2*B* and *C*, this asymmetry was also observed in mixed-type patches of deep cerebellar nuclei neurones and spinal cord neurones. In these patches, amplitude histograms showed three resolvable peaks (level 1, ~18 pS; level 2, ~38–40 pS; and level 3, ~50 pS; Fig. 2*B* and *C*). Levels 1 and 2 in these neurones were indistinguishable from those in Purkinje cell patches. While 2 → 1 transitions occurred more frequently

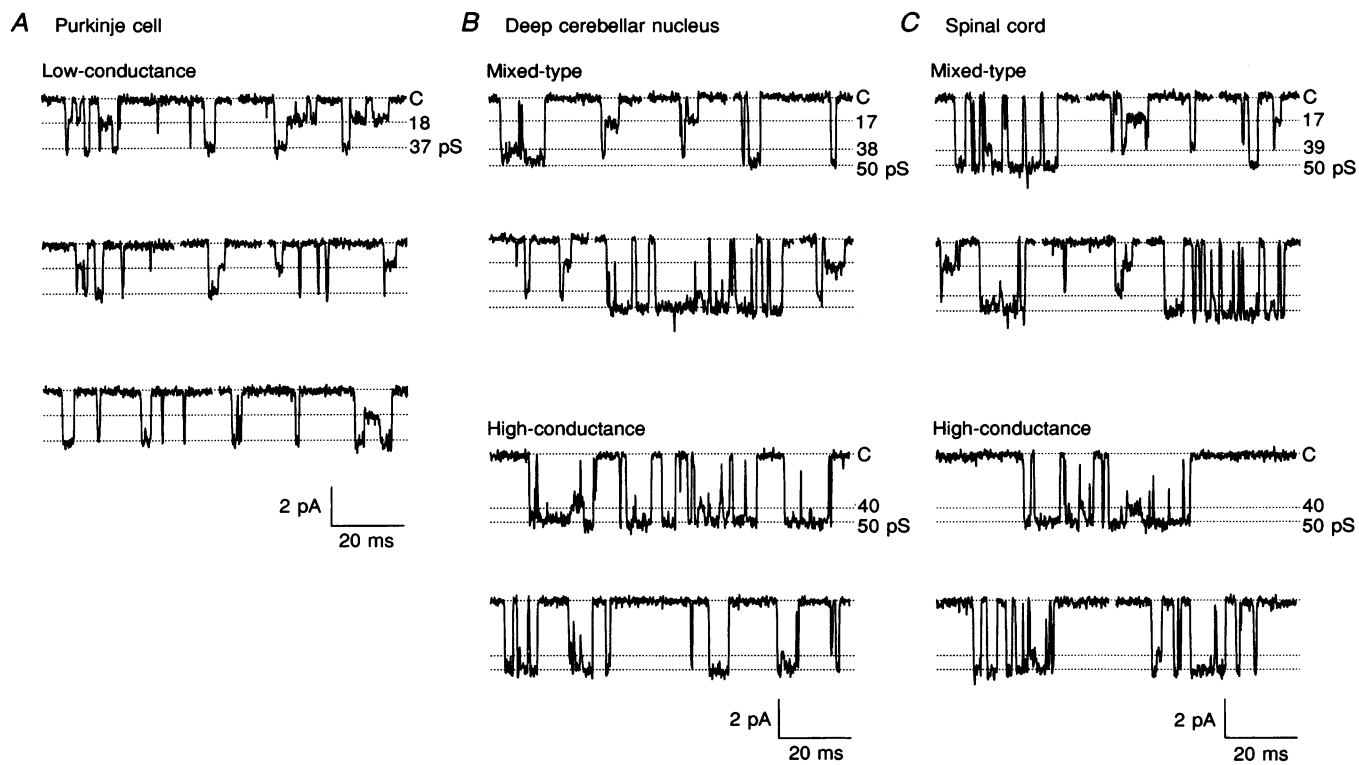

Figure 1. Examples of low- and high-conductance NMDA channels

NMDA channel openings activated in outside-out patches (−70 mV) from Purkinje cells, deep cerebellar nuclei neurones and dorsal horn spinal cord neurones. The various conductance levels (and closed state, C) are indicated by dotted lines. Glycine (10 μM) was present during all recordings. *A*, typical 37 and 18 pS openings activated by NMDA (30 μM) in a Purkinje cell patch (P4). Note the presence of clear direct transitions between the two levels. *B*, top two rows: NMDA (50 μM)-activated events in a 'mixed-type' patch from a neurone of the deep cerebellar nuclei (P4). Note the presence of openings to 17, 38 and 50 pS indicating the presence of both low- and high-conductance channels. *B*, bottom two rows: typical NMDA (50 μM)-activated 50 and 40 pS openings in a 'high-conductance' patch from another deep cerebellar nuclei neurone. *C*, top two rows: NMDA (10 μM)-activated 17, 39 and 50 pS events in a 'mixed-type' patch from a dorsal horn neurone of the spinal cord (P2). *C*, bottom two rows: NMDA (50 μM)-activated 50 and 40 pS events in a 'high-conductance' patch from another dorsal horn neurone.

than 1 → 2 transitions in both deep cerebellar nuclei and spinal cord neurones, the 2 → 3 transitions and 3 → 2 transitions occurred at similar frequencies. This asymmetry, which showed no apparent voltage dependence (between −30 and −90 mV; data not shown), suggests that the channel mechanism may not obey microscopic reversibility (see also Cull-Candy & Usowicz, 1987).

We have also examined patches which contained only NMDA events of the 50/40 pS type. As shown in Fig. 3, high-conductance NMDA-events revealed symmetrical open–open transitions between 40 and 50 pS levels (50·7 ± 0·5% from 50 to 40 pS, $n = 3$, dorsal horn neurones of the spinal cord; see also Stern *et al.* 1992). Thus the lack of asymmetry in the 50–40 pS transitions, observed in mixed-type patches, was also apparent in patches containing only 50/40 pS channels.

Table 1 presents our quantitative analysis of the proportion of transitions between the various possible states (including the closed state, C) for mixed-type patches; the data are grouped into six transition types. As described above, events with conductances in the range of roughly 38–40 pS are lumped together (level 2). We found that the density of high- and low-conductance channels varied between patches, since the percentage of openings to 18 and 50 pS differed widely. In all mixed-type patches from these neurones the high-conductance NMDA events predominated. Patches depicted in Table 1 were the ones that exhibited the highest frequency of openings of low-conductance channels of all the mixed-type patches examined. As a consequence, in Table 1, transitions of the type 2 ⟷ 3 are more frequent than transitions of the type 1 ⟷ 2. The main feature apparent in Table 1 is the lack of transitions

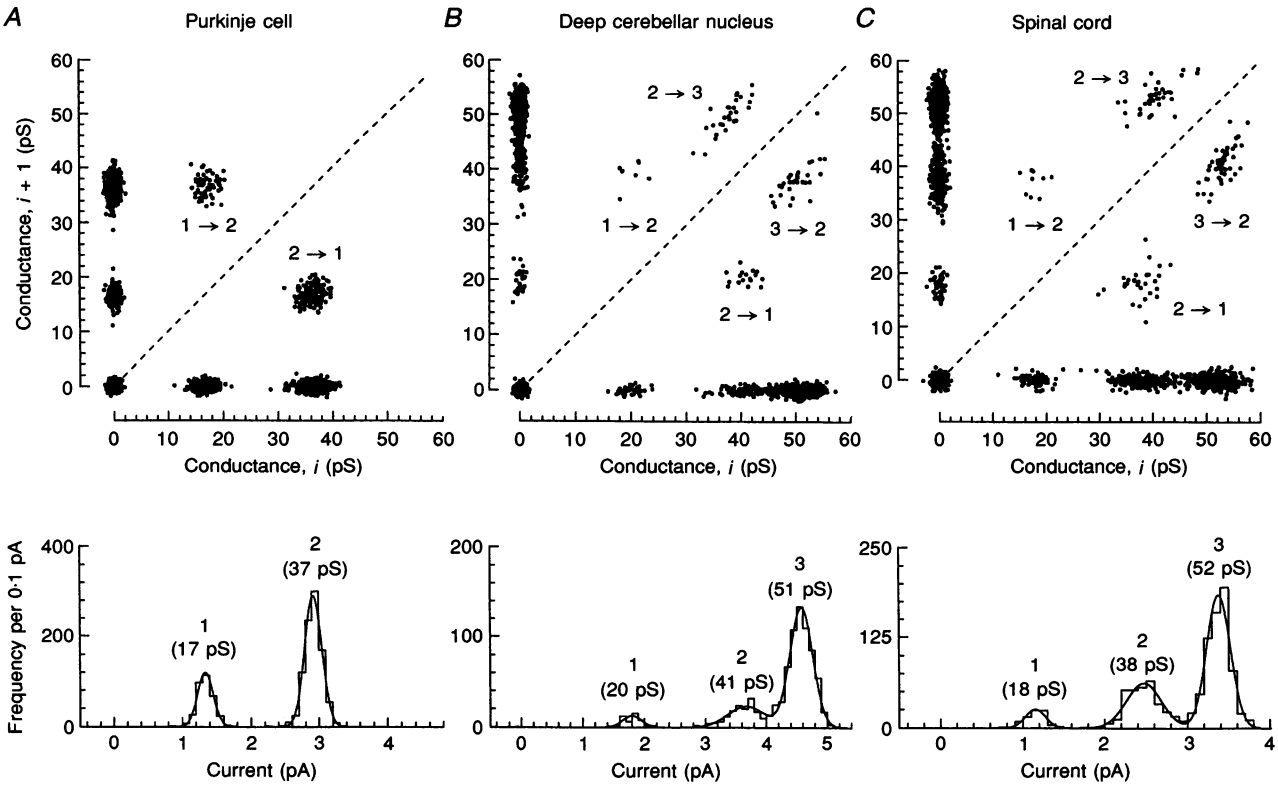

Figure 2. Transitions between conductance levels of NMDA channels

The graphs in the top panels illustrate the frequency of occurrence of transitions between two consecutive conductance levels (including the closed state) in outside-out patches from Purkinje cells, deep cerebellar nuclei neurones and dorsal horn neurones. Dots above the dashed diagonal lines represent transitions of C (closed) → level 1 (18 pS), C → level 2 (38/40 pS), C → level 3 (50 pS), 1 → 2 and 2 → 3, all being in opening directions. Dots below the dashed lines represent transitions of 3 → C, 2 → C, 1 → C, 3 → 2, and 2 → 1, all being in closing directions. There is scatter of conductance levels except closed state, as expected from the corresponding single-channel amplitude histograms (lower panels). A random Gaussian variable (S.D. = 0·05 pA) was added to all zero conductance levels, to prevent transitions to or from zero conductance levels appearing as a line. The degree of this artificially added scatter is displayed at the origin of each dashed line. Note that 2 → 1 transitions (steps from 38 to 18 pS) greatly exceeded the occurrence of 1 → 2 transitions (18 to 38 pS) in all cell types. Corresponding amplitude histograms (lower panels) were fitted with the sum of two Gaussian distributions (*A*) for openings in a Purkinje cell patch (P5; holding potential (V_h) = −80 mV; [NMDA], 50 μM), or three Gaussians (*B* and *C*) in mixed-type patches from a deep cerebellar nuclei neurone (P4; V_h = −90 mV; [NMDA], 50 μM) and a dorsal horn neurone of the spinal cord (P2; V_h = −65 mV; [NMDA], 10 μM).

Table 1. Analysis of types of transitions between conductance levels of NMDA receptors in mixed-type patches from deep cerebellar and spinal cord neurones

Transition	Deep cerebellar nucleus ($n = 1353$)	Spinal cord ($n = 1504$)
C ⟷ 1	4·4%	4·8%
C ⟷ 2	14·3%	23·2%
C ⟷ 3	75·2%	65·4%
1 ⟷ 2	1·9%	2·3%
2 ⟷ 3	4·2%	4·3%
1 ⟷ 3	0	0

Possible transitions are grouped into the 6 combinations: C (closed) ⟷ 1 (18 pS), C ⟷ 2 (38/40 pS), C ⟷ 3 (50 pS), 1 ⟷ 2, 2 ⟷ 3, 1 ⟷ 3. Each combination includes transitions in both directions. Note the absence of transitions between conductance levels 1 (18 pS) and 3 (50 pS) in both cell types.

between ~18 pS and the ~50 pS level (1 ⟷ 3). This observation adds further weight to the suggestion that the low-conductance channel is a distinct type of receptor, which occurs in isolation in Purkinje cells or co-exists with the high-conductance channels in neurones of the deep cerebellar nuclei and the spinal cord.

From *in situ* hybridization data, Purkinje cells possess mRNA for only NR2D and NR1 at this age (Akazawa *et al.* 1994; but see also Watanabe *et al.* 1994*b*), while deep cerebellar nuclei neurones and spinal cord neurones also possess mRNA for other NR2 subunits (NR2A and NR2B in the case of deep cerebellar nuclei neurones, and NR2B in dorsal horn neurones of spinal cord; Akazawa *et al.* 1994; Monyer *et al.* 1994). Therefore in these neurones it seems likely that the presence of the NR2D subunit is essential for the formation of low-conductance NMDA channels, while either NR2A or NR2B subunits (or both) are required to give 50/40 pS channel openings (see also Stern *et al.* 1992 for recombinant receptors). The 50/40 pS openings in deep cerebellar nuclei neurones and spinal cord neurones (Fig. 1*B* and *C*) were indistinguishable from those in immature cerebellar granule cells in thin slices (Fig. 6; see also Farrant *et al.* 1994) or indeed from those described previously in other cell types (e.g. Nowak, Bregestovski, Ascher, Herbet & Prochiantz, 1984). Since it was not possible to discriminate between conductances of ~38 and ~40 pS (in patches where 38/18 pS openings and 50/40 pS openings were both present), low-conductance channels could be accurately characterized only in patches that lacked high-conductance events. For this reason, we have focused our analysis on the NMDA channels in Purkinje cells.

Pharmacology of the low-conductance NMDA response

It was necessary to determine that the low-conductance channels in Purkinje cell patches exhibited the pharmacological properties expected of NMDA receptors, since evidence for NMDA receptors in these cells *in situ* has previously been equivocal. As illustrated in Fig. 4*A*, the response to 50 μM NMDA (with 10 μM glycine) was reversibly suppressed by the competitive NMDA antagonist D-2-amino-5-phosphonopentanoic acid (D-AP5; 50 μM). Furthermore, the currents were completely blocked by the competitive glycine site antagonist 7-chlorokynurenate (30 μM, in the presence of 3 μM glycine; Fig. 4*B*). At a potential of −70 mV, 1 mM extracellular Mg^{2+} produced an almost complete block of channel openings which reappeared at more positive potentials (Fig. 4*C*).

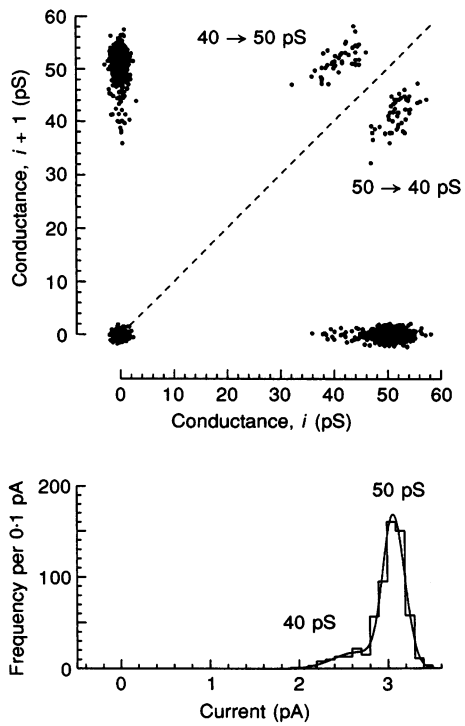

Figure 3. Transitions between conductance levels of high-conductance NMDA channels

The graph in the top panel illustrates the frequency of occurrence of transitions between the closed state, 40 pS and 50 pS levels in a patch from a spinal cord dorsal horn neurone (P2) containing only high-conductance NMDA openings. Dots above the dashed line represent transitions of C (closed) → 40 pS, C → 50 pS, 40 → 50 pS. Dots below the dashed line represent transitions of 50 pS → C, 40 pS → C, 50 → 40 pS. Note equal occurrence of transitions of 40 → 50 pS and 50 → 40 pS. The bottom panel shows the corresponding amplitude distribution of single-channel currents ($V_h = -60$ mV; [NMDA], 10 mM).

Glutamate (1–100 μM, with 10 μM glycine) activated openings of similar amplitude, which were also blocked by D-AP5 (100 μM). The degree of block by D-AP5 (as measured by reduction of charge transfer through single NMDA channels activated by 100 μM glutamate; 90 ± 2%; $n = 4$) was not significantly different ($P > 0.05$) from that seen in granule cells (92 ± 3%; $n = 4$), despite the existence of different NMDA receptor types in these cells (Akazawa *et al.* 1994; Farrant *et al.* 1994). Interestingly, recombinant $\zeta 1/\epsilon 4$ NMDA receptors (the mouse equivalent of NR1/NR2D) are reported to be markedly less sensitive to block by D-AP5 than other subunit pairs (Ikeda *et al.* 1992; Kutsuwada *et al.* 1992).

Similarly, in patches from deep cerebellar nuclei neurones and spinal cord neurones, NMDA channels were blocked by extracellular Mg^{2+} (1 mM, $V_h = -60$ mV) in a voltage-dependent manner (data not shown), confirming that both low- and high-conductance channel openings resulted from the activation of NMDA receptors in these neurones.

Single-channel properties of NMDA receptors in Purkinje cells

As shown in Fig. 5*A*, amplitude distributions for NMDA channels in Purkinje cells revealed two distinct levels (see also Fig. 2*A*). Slope conductance values were determined by recording single-channel currents at three to five potentials (−100 to −20 mV). In the patch depicted in Fig. 5*B* the slope conductances of the two levels were 37 and 17 pS; the mean values obtained were 37·9 ± 1·1 and 17·8 ± 0·7 pS ($n = 7$ patches). The 38 pS level accounted for 80·8 ± 1·0% of all openings ($n = 15$). The relative proportion of 18 pS and 38 pS levels was consistent between patches, supporting the idea that they arose from the same channel (rather than two separate channels). The channel conductances and relative proportion of the two levels obtained with glutamate (1–10 μM) and aspartate (10 μM) were indistinguishable from those obtained with NMDA (data not shown).

While the single-channel conductance levels of these low-conductance NMDA receptors were in the same range as those of putative NR2C-containing receptors in mature cerebellar granule cells in slices (Farrant *et al.* 1994) and of recombinant NR1/NR2C channels (Stern *et al.* 1992), there were clear differences in their kinetic properties and transition patterns. Thus, while the mean apparent open times for the main and subconductance levels were almost identical for recombinant NR1/NR2C channels (0·61 ms for both levels; Stern *et al.* 1992), this was not the case for the

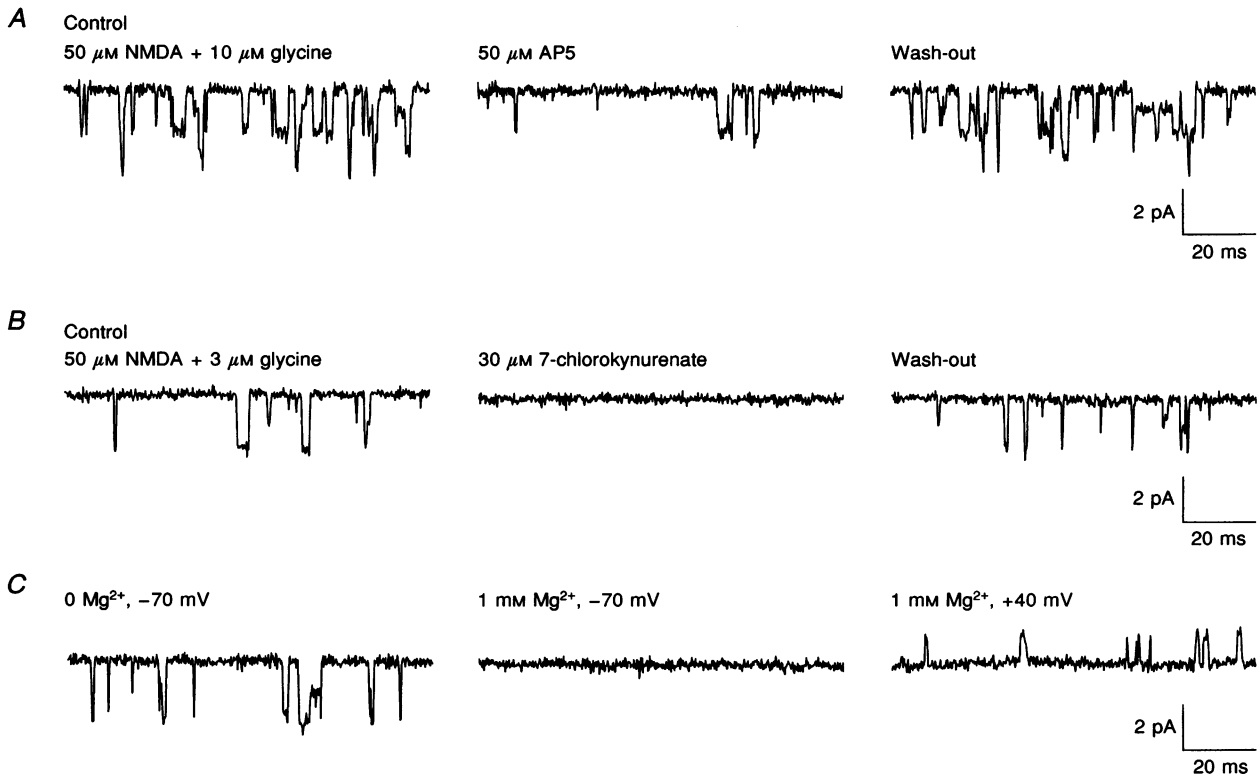

Figure 4. Pharmacology of the NMDA receptor channels in Purkinje cells

A, reduction in the frequency of low-conductance NMDA channel openings by AP5 (50 μM). Occasional overlap of multiple openings were apparent in the absence of AP5. $V_h = -60$ mV; [NMDA], 50 μM; [glycine], 10 μM. *B*, block of low-conductance NMDA channel openings by 7-chlorokynurenate (30 μM). $V_h = -60$ mV; [NMDA], 50 μM; [glycine], 3 μM. *C*, low-conductance NMDA channels were blocked by 1 mM Mg^{2+} at −70 mV, which was relieved at +40 mV. [NMDA], 50 μM; [glycine], 10 μM. Recordings in *A*–*C* were obtained from different patches.

NMDA channels in Purkinje cells. Figure 5*C* and *D* shows open time distributions for the main and subconductance state of Purkinje cell NMDA channels ($V_h = -60$ mV); in this patch single exponentials fitted to the distributions gave a mean apparent open time of 0·75 ms for the main conductance and 1·14 ms for the subconductance. The mean values obtained were 0·74 ± 0·07 ms ($n = 4$) for the 38 pS level, and 1·27 ± 0·18 ms ($n = 4$) for the 18 pS conductance. The mean open time of the subconductance was thus significantly longer ($P < 0·05$, paired t test). Furthermore, the asymmetry of the 38/18 pS transitions in Purkinje cells, deep cerebellar nuclei neurones and spinal cord neurones contrasts with the situation described for recombinant NR1/NR2C channels which do not exhibit this behaviour. The percentage of transitions (of all transitions between two consecutive levels) were 1·5% (18 → 38 pS) and 3·8% (38 → 18 pS) in Purkinje cell NMDA channels ($n = 13$ patches), whereas they were 4·8% (19 → 36 pS) and 5·3% (36 → 19 pS) in recombinant NR1/NR2C channels (Stern *et al.* 1992). This asymmetry could therefore prove a useful diagnostic feature for native NR2D-containing channels whose channel mechanism may not obey microscopic reversibility.

Low-conductance NMDA channels have a reduced sensitivity to extracellular Mg^{2+}

Recombinant NMDA receptors composed of NR1/NR2A or NR1/NR2B subunits have been shown to display a higher sensitivity to block by extracellular Mg^{2+} than those formed by NR1/NR2C or NR1/NR2D subunits (Monyer *et al.* 1994). To determine whether this functionally important aspect of NMDA receptors may also differ between native NMDA receptor subtypes, we have compared the Mg^{2+} sensitivity of low-conductance NMDA receptors in Purkinje cells (P1–5) with that of high-conductance NMDA receptors in cerebellar granule cells (P5–8). The latter have single-channel properties similar to those of recombinant NR1/NR2A or NR1/NR2B subunit combinations (Farrant *et al.* 1994), consistent with the *in situ* hybridization data which indicates the presence of these subunits (Akazawa *et al.* 1994; Monyer *et al.* 1994).

While Purkinje cells had the advantage of expressing a population of low-conductance NMDA channels in isolation, they had an extremely low NMDA current density (whole-cell current density < −2·5 pA pF^{-1} in 100 μM NMDA at −60 mV). This was far too small to allow us to record

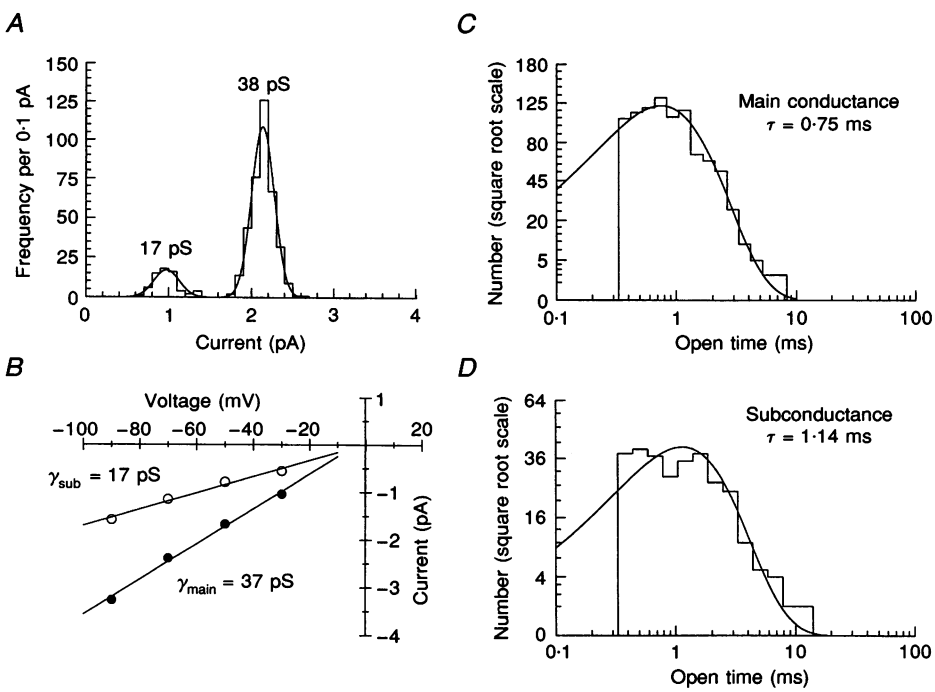

Figure 5. Single-channel properties of low-conductance NMDA channels in Purkinje cell patches
A, amplitude distribution of cursor-fitted single-channel currents ($V_h = -60$ mV) from an outside-out patch (P5). The distribution was fitted with the sum of two Gaussian components with mean chord conductances of 17 and 38 pS. Relative proportion of openings to the 38 pS levels (expressed as the area under the curve) was 84·9% in this example. *B*, current–voltage relationship of the main and subconductance levels of NMDA channels in another Purkinje cell patch (P4). Closed and open circles indicate main (37 pS) and subconductance (17 pS) levels, respectively. Slope conductance values were obtained by linear regression; extrapolated reversal potential, −2·3 mV. *C* and *D*, open time distributions of the main level (*C*) and the subconductance level (*D*) of NMDA channels in a Purkinje cell patch (P1). Number of events are expressed in square root scale. Each distribution was fitted by a single exponential with a time constant of 0·75 ms for the main level and 1·14 ms for the subconductance level. The resolution was 332 μs (2 × filter rise times) for channel openings, and 170 μs for channel closures. $V_h = -60$ mV; [NMDA], 50 μM, [glycine], 10 μM.

NMDA currents that generated measurable current–voltage relationships in the presence of Mg^{2+}. To determine the Mg^{2+} sensitivity of the channels it was therefore necessary to measure the integral of the NMDA single-channel currents, i.e. the charge transfer at one holding potential (−60 mV). The concentration of Mg^{2+} was set at 0·1 mM to preserve measurable channel activity in the presence of Mg^{2+} and hence allow us to quantify the blocking effect of Mg^{2+}.

Figure 6 illustrates the effect of 0·1 mM Mg^{2+} on NMDA-induced single-channel currents in outside-out patches from a Purkinje cell (Fig. 6*A* and *B*) and a granule cell (Fig. 6*C* and *D*). Channel openings were briefer in both cell types (at −60 mV) in Mg^{2+} solution. However, as is apparent in Fig. 6*C*, the channel block was visibly more pronounced for 50 pS NMDA channels in granule cells. In Fig. 6*B* and *D* the total charge transferred during each 100 ms of NMDA channel activity is indicated as a single point (in 0 Mg^{2+} and in 0·1 mM Mg^{2+}). The mean value of these measurements (during a 30 s recording period) was used as an indicator of NMDA channel activity in the absence and presence of Mg^{2+}. As shown in Fig. 6*B*, the charge transfer through low-conductance NMDA channels in Purkinje cells was reduced by only 31·5% in 0·1 mM Mg^{2+} (on average by 33·9 ± 1·8%, $n = 6$), while that through the 50/40 pS channels in granule cells (Fig. 6*D*) was decreased by 76·8% under similar conditions (on average by 81·5 ± 2·6%, $n = 5$).

The differential Mg^{2+} sensitivity of NMDA channels in Purkinje and granule cells was also evident in the distribution of mean apparent open times. Extracellular Mg^{2+} acts as an open channel blocker and produces rapid closing and reopening of NMDA channels (Nowak *et al.* 1984; Ascher & Nowak, 1988). Figure 7 illustrates the effect of 0·1 mM Mg^{2+} on the open time distributions of the main conductance levels of NMDA channels in a Purkinje cell patch (Fig. 7*A*) and a granule cell patch (Fig. 7*B*). In this example, the open time was reduced from 0·51 ms (in nominally Mg^{2+}-free solution) to 0·26 ms (in 0·1 mM Mg^{2+}) in the Purkinje cell, and from 3·2 ms to 0·35 ms in the granule cell. The mean values for the apparent open times in nominally Mg^{2+}-free solution and 0·1 mM Mg^{2+} were, respectively, 0·63 ± 0·07 ms and 0·33 ± 0·04 ms ($n = 6$; −60 mV) in Purkinje cells, and 3·49 ± 0·44 ms and 0·43 ± 0·04 ms ($n = 3$) in granule cells (see also Nowak *et al.* 1984; Tsuzuki, Mochizuki, Iino, Mori, Mishina & Ozawa, 1994). Thus, Mg^{2+} was markedly less effective at blocking the low-conductance NMDA channels in Purkinje cell patches. Figure 8 shows the dramatic difference in Mg^{2+} sensitivity of NMDA channels recorded in Purkinje cells and granule cells.

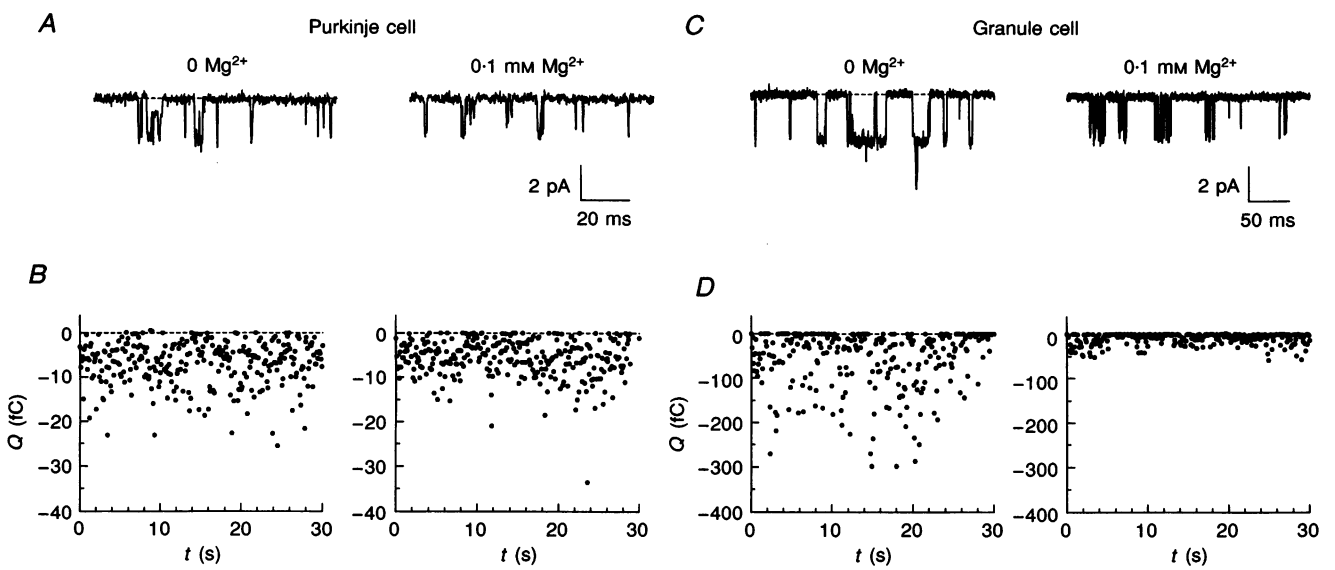

Figure 6. Mg^{2+} block of high- and low-conductance NMDA channels

A, single-channel currents in an outside-out patch from a Purkinje cell (P3), in Mg^{2+}-free (left) and in 0·1 mM Mg^{2+} (right) solutions. *C*, single-channel currents in an outside-out patch from a cerebellar granule cell (P6) in Mg^{2+}-free (left) and in 0·1 mM Mg^{2+} (right) solutions. Note the different time scale for the single-channel recordings in *A* and *C*. *B* and *D*, total charge transfer (*Q*, in femtocoulombs) through NMDA channel openings during a 30 s period in the absence (left panels) and presence (right panels) of Mg^{2+}; each dot represents the charge transfer through NMDA channel openings during a 100 ms epoch. Care was taken to use only those records obtained from patches displaying stable channel activity during entire recording periods. Because of their higher conductances and longer open times, the charge transfer through 50/40 pS NMDA channels in granule cells was much larger than that through 38/18 pS channels in Purkinje cells. Data in Mg^{2+} were obtained 2 min after Mg^{2+} application. The degree of block, obtained from the ratio of average charge transfer in the presence and absence of Mg^{2+}, was 31·5% (Purkinje cell) and 76·8% (granule cell) in these examples. $V_h = -60$ mV; [NMDA], 50 μM; [glycine], 10 μM in *A*–*D*.

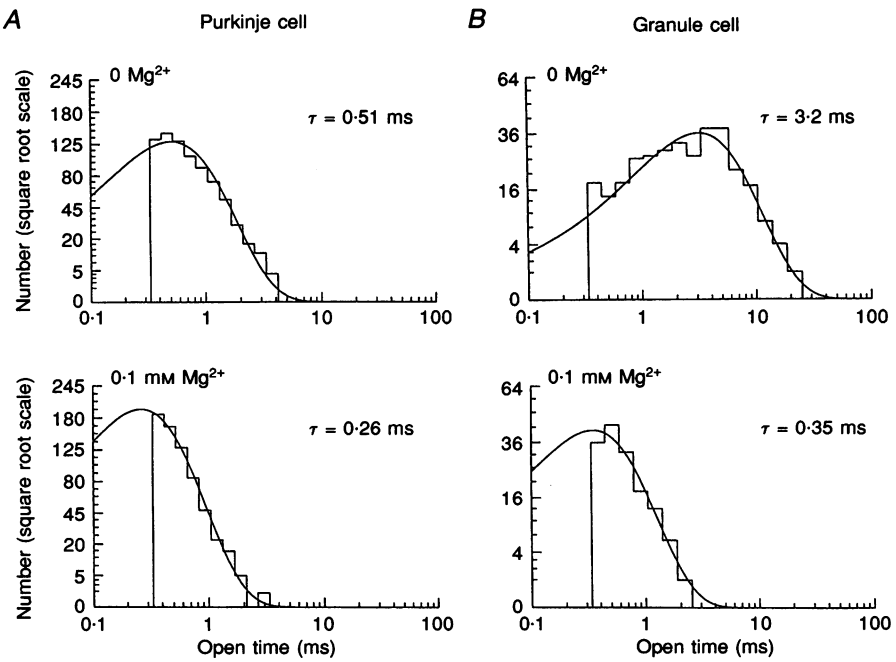

Figure 7. Effect of 0·1 mM Mg^{2+} on open time of high- and low-conductance NMDA channels

Representative open time distributions of NMDA channels in a Purkinje cell (*A*) and a granule cell (*B*), in the absence and presence of 0·1 mM Mg^{2+}. $V_h = -60$ mV. Only openings to the main conductance level were included in the histograms. In the absence and presence of 0·1 mM Mg^{2+}, the mean apparent open times (the time constant of single exponential fit) was 0·51 ms and 0·26 ms, respectively, in the Purkinje cell patch, and 3·2 ms and 0·35 ms, respectively, in the granule cell patch.

Time course of expression of low-conductance NMDA channels in Purkinje cells

The graph in Fig. 9 illustrates the percentage of Purkinje cell patches that gave detectable NMDA single-channel currents during the first 12 days of postnatal development. At P1, about 70% of patches responded to NMDA; between P4 and P6, channel activity was observed in about 90% of patches. In older animals (P8–10), we often failed to detect NMDA channel activity, indicating a decline in the expression level of NMDA receptors. At P12, none of the Purkinje cell patches responded to NMDA. This correlates well with the time course of expression of mRNA for the NR2D subunit in Purkinje cells in the rat (Akazawa *et al.* 1994). Identification of NR2D-containing receptors in neonatal Purkinje cells has thus resolved one of the questions arising from previous studies on these cells. The developmental decline in expression of functional NMDA receptors in Purkinje cells explains why NMDA receptors were not seen in patch-clamp studies from older animals (from 8 days to 6 weeks old; Perkel, Hestrin, Sah & Nicoll, 1990; Farrant & Cull-Candy, 1991; Llano, Marty, Armstrong & Konnerth, 1991; but see Crepel & Audinat, 1991).

DISCUSSION

Our experiments have identified the presence of a novel type of native low-conductance NMDA receptor with distinct channel properties, associated with expression of mRNA for the NR2D subunit. Our observations have several broad implications for native NMDA receptors. First, they provide evidence that *functional diversity* of native NMDA receptors is probably widespread in the CNS –

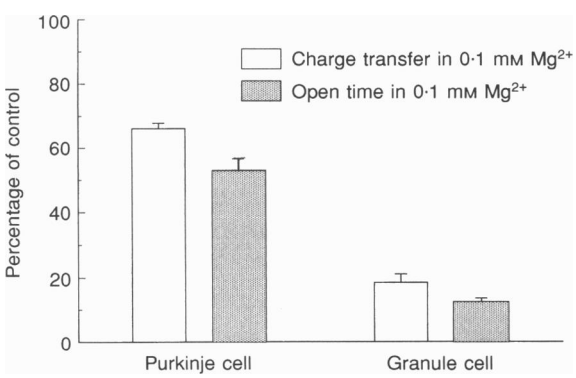

Figure 8. Summary of the Mg^{2+} block of low-conductance NMDA channels in Purkinje cells was less marked than block of 50/40 pS channels in cerebellar granule cells

Effect of 0·1 mM Mg^{2+} on high- and low-conductance NMDA channels, measured as a change in charge transfer (open columns), or a change in mean open time (shaded columns). Vertical error bars represent S.E.M. Data on the left are from low-conductance channels in Purkinje cells, data on the right from high-conductance channels in cerebellar granule cells. $V_h = -60$ mV.

given the extensive distribution of NR2D mRNA revealed by *in situ* hybridization (Monyer *et al.* 1994). Second, they demonstrate that these low-conductance NMDA receptors have properties that are distinct from the 50/40 pS type of NMDA receptor that has previously been studied in detail (reviewed by Ascher & Johnson, 1994; McBain & Mayer, 1994). Third, our observations provide a simple interpretation of the multiple conductance levels associated with NMDA receptors in earlier studies (Jahr & Stevens, 1987; Cull-Candy & Usowicz, 1987, 1989). And last, the marked similarity in single-channel properties of putative NR1/NR2D receptors with the previously identified NR1/NR2C receptors (Farrant *et al.* 1994; see also Stern *et al.* 1992) suggests that a functionally distinct subclass of NMDA receptors exists within the CNS. These various aspects are considered below.

Subunit composition of low-conductance NMDA channels

The expression pattern of mRNA for NMDA receptor subunits is consistent with the idea that the low-conductance channels we have examined contain NR1 and NR2D subunits. *In situ* hybridization studies of neonatal rat cerebellum have indicated that mRNA for the NR2D subunit is expressed in Purkinje cells from birth to P8, but it is no longer detectable by P11 (Akazawa *et al.* 1994). During this time the only other NMDA receptor subunit detected in rat Purkinje cells is NR1 (Akazawa *et al.* 1994; Monyer *et al.* 1994) which is required for the efficient formation of functional receptors. In the case of Purkinje cells, the 38/18 pS openings must arise from NMDA receptors containing only NR1 and NR2D subunits. Low-conductance channels were also observed in deep cerebellar nuclei neurones and dorsal horn neurones of the spinal cord at a stage when these cells were expected to express mRNA for the NR2D subunit (Akazawa *et al.* 1994; Monyer *et al.* 1994). These cell types also express mRNAs for NR2A and/or NR2B, which are known to generate high-conductance channels when expressed as recombinant receptors (i.e. NR1/NR2A or NR1/NR2B; see Stern *et al.* 1992). Thus the presence of NR2A or NR2B (along with NR2D) does not preclude the formation of low-conductance channels in neurones. This is of interest as there is evidence that some native NMDA receptors may contain more than one type of NR2 subunit (see Wafford, Bain, Le-Bourdelles, Whiting & Kemp, 1993; Sheng, Cummings, Roldan, Jan & Jan, 1994). Given the independent behaviour of low- and high-conductance channels in neurones that express both types of channels, it seems likely that they are composed, respectively, of NR1/NR2D and NR1/NR2A (or NR1/NR2B).

It is known that mRNA for the NR2D subunit is no longer present in Purkinje cells at P11, while mRNA for the NR2A subunit appears at around P8 – albeit at a low level (Akazawa *et al.* 1994). However, this does not appear to result in the expression of functional receptor protein since there is a lack of antibody labelling for the NR2A (and NR2B) subunits in Purkinje cells of young rats (Petralia, Wang & Wenthold, 1994), and we were unable to detect 50/40 pS NMDA channels in any of the patches examined. A previous study by Rosenmund, Legendre & Westbrook (1992) described NMDA receptor channels in patches from enzymatically dissociated Purkinje cells (0- to 4-day-old rats) maintained for up to 24 h. At this stage the cells *in situ* are not expected to express NR2A. While a range of channel conductances were observed, the channels were indistinguishable from the high-conductance type of NMDA receptor with respect to channel open time and sensitivity to Mg^{2+} block. The explanation for this observation is not known.

An interpretation of earlier observations on multiple conductance NMDA channels

The present results demonstrate that low- and high-conductance single-channel openings reflect distinct types of NMDA receptors, and suggest that the low-conductance channels in deep cerebellar nuclei and spinal cord neurones are similar to those in Purkinje cells. This observation provides a simple interpretation of multiple conductance levels of NMDA receptors described in earlier studies (Jahr & Stevens, 1987; Cull-Candy & Usowicz, 1987, 1989; Ascher, Bregestovski & Nowak, 1988). Thus, it seems probable that the wide range of levels reflected the presence of high- and low-conductance channels. Indeed, in the case of cultured 'large cerebellar cells' (including Purkinje cells and deep cerebellar nuclei neurones; see Cull-Candy & Usowicz, 1987, 1989) several pieces of evidence favour the idea that the lower amplitudes can be ascribed to the

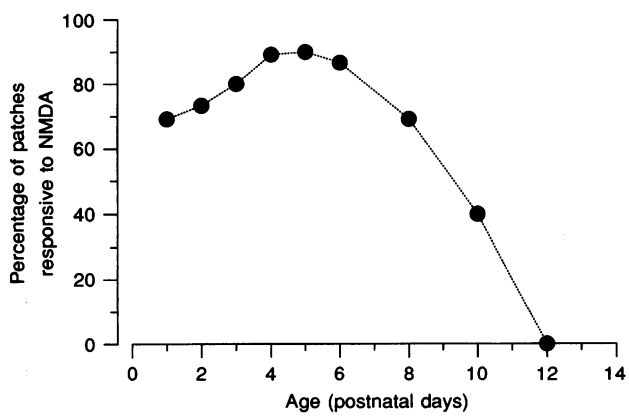

Figure 9. Age-dependent expression of NMDA receptor in Purkinje cells

Percentage of Purkinje cell patches which showed NMDA-activated channels at the various ages studied. Patches were exposed to 50 μM NMDA (with 10 μM glycine, $V_h = -60$ or -70 mV). The number of patches tested was 13 (P1), 15 (P2), 10 (P3), 37 (P4), 10 (P5), 15 (P6), 13 (P8), 10 (P10), 5 (P12). No response to NMDA was detected at P12.

presence of NR2D-containing receptors. First, the NMDA-activated conductance levels of 38 and 18 pS in 'large cerebellar neurones' were similar in amplitude to those identified in the present study, and also showed a high frequency of direct transitions. Second, the 38/18 pS steps showed time asymmetry similar to that described here; 38 to 18 pS steps made up 77% of all transitions between these levels, compared with 72% in the present study. Third, the 18 pS subconductance was markedly longer than the 38 pS openings. And fourth, few transitions were seen between the 50 and 18 pS levels. Similarly, NMDA-activated events of 35 and 16 pS observed in cultured embryonic mouse spinal neurones (Ascher *et al.* 1988) may have arisen from this type of channel (the mouse equivalent: ε4-containing receptor; see Ikeda, *et al.* 1992; Watanabe *et al.* 1994), given their conductance levels and their brief open times. However, the possibility previously suggested by Stern *et al.* (1992) that the lower multiple conductance levels in cultured large cerebellar cells could be ascribed to native NR1/NR2C-type channels now seems unlikely, given the clear difference of single-channel properties between NR2D- and NR2C-containing receptors.

The observation of a distinct type of low-conductance NMDA receptor allows a clearer physical interpretation of the multiple conductance levels of *native* NMDA receptors (reviewed by Cull-Candy, Farrant & Feldmeyer, 1995): 50/40 and 38/18 pS openings arise from separate high- and low-conductance channels, respectively.

Comparison with recombinant NMDA receptors: similarities and differences

In the light of evidence suggesting that certain properties of recombinant NMDA receptors may differ from their native counterparts (see below), any comparison of native and recombinant channels needs to be treated with caution. Nevertheless it is of interest that native low-conductance NMDA receptors and recombinant NR1/NR2D receptors exhibit some similarities and some differences. Thus, the putative NR2D-containing NMDA channels in Purkinje cells showed a reduced sensitivity to Mg^{2+} (when compared with putative NR1/NR2A- and NR1/NR2B-containing receptors in granule cells), as previously described for the recombinant NR1/NR2D receptor (Monyer *et al.* 1994). It is of note that the low-conductance channel in the present study and the recombinant NR1/NR2C channels, both of which have a low sensitivity to Mg^{2+} block (when compared with NR1/NR2A or NR1/NR2B channels: Monyer *et al.* 1994), also have brief open times (see also Stern *et al.* 1992; Farrant *et al.* 1994).

One of the characteristic features of recombinant NR2D receptors is their slow deactivation kinetics (Monyer *et al.* 1994). If this property also applied to native NR2D-containing receptors, it could be of physiological importance since it would result in prolonged activation of the channels. Unfortunately, deactivation kinetics of NMDA channels could not be measured from the averaged whole-cell glutamate responses in Purkinje cells as the current density in these cells was too small. This precluded direct comparison with the recombinant data. However, it was clear that NMDA channel activity in Purkinje cell patches disappeared within 100 ms of removal of rapidly applied glutamate (100 μM glutamate, with 10 μM glycine, 500 ms pulse; A. Momiyama, D. Feldmeyer & S. G. Cull-Candy, unpublished observations), and certainly more rapidly than expected from the results described for recombinant NR1/NR2D receptors. Thus, the possibility exists of a difference in the deactivation kinetics of native and recombinant NR1/NR2D receptors, although apparent differences could have resulted from variation in experimental conditions. A further complication could arise if the splice variants of NR1 or NR2D subunits (Ishii *et al.* 1993; McBain & Mayer, 1994) differ in their deactivation kinetics. This feature of the isoforms has yet to be compared, and the identity of NR1 and/or NR2D splice variant in Purkinje cells is not known. It is therefore too early to draw conclusions on the time course of channel closure for this type of native low-conductance channel.

Despite some apparent differences between the recombinant NR1/NR2D channels and the channels in Purkinje cells, they exhibit an important similarity. Recent experiments have indicated that single recombinant NR1/NR2D channels have conductance levels almost identical to those described here (Wyllie, Béhé, Edmonds, Nassar, Schoepfer & Colquhoun, 1996).

Possible functional considerations

Current flow through 50/40 pS NMDA receptors is substantially suppressed by extracellular Mg^{2+} ions at resting potential (Nowak *et al.* 1984; Mayer, Westbrook & Guthrie, 1984) resulting in a voltage-dependent, and hence activity-dependent, Ca^{2+} entry through these channels. From the I–V relationship described for recombinant NMDA receptors (see Monyer *et al.* 1994), it seems likely that at physiological Mg^{2+} concentrations (~1 mM) a relatively weak depolarization would be sufficient to permit Ca^{2+} influx in neurones possessing NR1/NR2D receptors – as a result of their low sensitivity to extracellular Mg^{2+}. While it was not possible to measure the Mg^{2+} sensitivity of low-conductance NMDA channels in cells expressing a mixed NMDA receptor population, it seems likely that the low-conductance channels in deep cerebellar nuclei neurones and spinal cord neurones will also exhibit a low Mg^{2+} sensitivity. The possibility of mixed populations of NMDA channels (with high and low sensitivity to Mg^{2+}) at synapses could allow for considerable diversity in activity-dependent fractional Ca^{2+} flux during excitatory synaptic transmission.

NMDA receptor-mediated currents have not been detected during EPSCs in Purkinje cells (Perkel *et al.* 1990; Llano *et al.* 1991), even in cells from young animals at a stage when they are expressing somatic NMDA receptors (P2–P6: A. Momiyama, D. Feldmeyer & S. G. Cull-Candy, unpublished observations). However, the emergence of

NMDA receptors in these cells at a stage when dramatic developmental changes are occurring raises the possibility that the extrasynaptic NMDA channels may be linked to these developmental processes. The extensive expression of mRNA for the NR2D subunit in the embryonic brain seems to be in accord with this idea (Monyer *et al.* 1994). Interestingly, activation of NMDA receptors has been implicated in the elimination of the multiple innervation of Purkinje cells by climbing fibres (see Rabacchi, Bailly, Delhaye-Bouchaud & Mariani, 1992), which takes place between P5 and P15 (Crepel, Delhaye-Bouchaud & Dupont, 1981; Mariani & Changeux, 1981), and is inhibited by the NMDA antagonist D,L-AP5. The developmental decrease in the level of NMDA channel activity (Fig. 9) and the elimination of multiple climbing fibre innervation (Crepel *et al.* 1981; Mariani & Changeux, 1981) show a strikingly similar time course.

Low-conductance channels: a functionally distinct class of NMDA receptor

A low-conductance NMDA channel, distinct from the one described here, has previously been identified in mature rat cerebellar granule cells (Farrant *et al.* 1994). These receptors exhibit single-channel properties that match those of the recombinant NR1/NR2C receptors (Stern *et al.* 1992). Furthermore, the expression of these low-conductance channels coincides with the appearance of mRNA for the NR2C subunit (Akazawa *et al.* 1994; Monyer *et al.* 1994; Farrant *et al.* 1994). At the single-channel level, these putative NR1/NR2C receptors can be clearly distinguished from the low-conductance channels in Purkinje cells, on the basis of the mean apparent open time of their subconductance (which is briefer than for the Purkinje cell receptor) and in the absence of asymmetry in the transitions between the conductance levels (see Stern *et al.* 1992). However, our results reveal similarities between putative NR1/NR2D receptors and NR1/NR2C receptors in their single-channel conductance levels, in the brief mean open times of their main levels (see Stern *et al.* 1992; Farrant *et al.* 1994) and in their low sensitivity to block by extracellular Mg^{2+} (Monyer *et al.* 1994). We therefore propose that low-conductance channels associated with NR2C or NR2D subunits represent a subclass of NMDA receptors *functionally distinct* from the widespread high-conductance channels. Interestingly, this separation of NMDA receptors into two functional subclasses mirrors certain structural properties of the NR2 subunits. Thus, similarity in size and amino acid sequence is greatest between NR2A and 2B, and between NR2C and 2D (Ishii *et al.* 1993).

Akazawa, C., Shigemoto, R., Bessho, Y., Nakanishi, S. & Mizuno, N. (1994). Differential expression of five *N*-methyl-D-aspartate receptor subunit mRNAs in the cerebellum of developing and adult rats. *Journal of Comparative Neurology* **347**, 150–160.

Ascher, P., Bregestovski, P. & Nowak, L. (1988). *N*-methyl-D-aspartate-activated channels of mouse central neurones in magnesium-free solutions. *Journal of Physiology* **399**, 207–226.

Ascher, P. & Johnson, J. W. (1994). The NMDA receptor, its channel, and its modulation by glycine. In *The NMDA Receptor*, 2nd edn, ed. Collingridge, G. L. & Watkins, J. C., pp. 177–205. Oxford University Press, Oxford.

Ascher, P. & Nowak, L. (1988). The role of divalent cations in the *N*-methyl-D-aspartate responses of mouse central neurones in culture. *Journal of Physiology* **399**, 247–266.

Carmignoto, G. & Vicini, S. (1992). Activity-dependent decrease in NMDA receptor responses during development of the visual cortex. *Science* **258**, 1007–1011.

Colquhoun, D. & Sigworth, F. J. (1995). Fitting and statistical analysis of single-channel records. In *Single-Channel Recording*, 2nd edn, ed. Sakmann, B. & Neher, E., pp. 483–587. Plenum Press, New York.

Crepel, F. & Audinat, E. (1991). Excitatory amino acid receptors of cerebellar Purkinje cells: development and plasticity. *Progress in Biophysics and Molecular Biology* **55**, 31–46.

Crepel, F., Delhaye-Bouchaud, N. & Dupont, J. L. (1981). Fate of the multiple innervation of cerebellar Purkinje cells by climbing fibers in immature control, x-irradiated and hypothyroid rats. *Developmental Brain Research* **1**, 59–71.

Cull-Candy, S. G., Farrant, M. & Feldmeyer, D. (1995). NMDA channel conductance: a user's guide. In *Excitatory Amino Acids and Synaptic Transmission*, ed. Wheal, H. V. & Thompson, A. M., pp. 121–132. Academic Press, London.

Cull-Candy, S. G., Howe, J. R. & Usowicz, M. M. (1987). Single glutamate-receptor channels in two types of cerebellar neurones. In *Excitatory Amino Acids in Health and Disease*, ed. Lodge, D., pp. 165–185. Wiley, London.

Cull-Candy, S. G. & Usowicz, M. M. (1987). Multiple-conductance channels activated by excitatory amino acids in cerebellar neurons. *Nature* **325**, 525–528.

Cull-Candy, S. G. & Usowicz, M. M. (1989). On the multiple-conductance single channels activated by excitatory amino acids in large cerebellar neurones of the rat. *Journal of Physiology* **415**, 555–582.

Farrant, M. & Cull-Candy, S. G. (1991). Excitatory amino acid receptor-channels in Purkinje cells in thin cerebellar slices. *Proceedings of the Royal Society* B **244**, 179–184.

Farrant, M., Feldmeyer, D., Takahashi, T. & Cull-Candy, S. G. (1994). NMDA-receptor channel diversity in the developing cerebellum. *Nature* **368**, 335–339.

Feldmeyer, D., Farrant, M. & Cull-Candy, S. G. (1995). Macroscopic kinetic properties of NMDA receptors in patches from granule cells of the rat cerebellum. *Journal of Physiology* **489.P**, 14*P*.

Hestrin, S. (1992). Developmental regulation of NMDA receptor-mediated synaptic currents at a central synapse. *Nature* **357**, 686–689.

Hollmann, M., Boulter, J., Maron, C., Beasley, L., Sullivan, J., Pecht, G. & Heinemann, S. (1993). Zinc potentiates agonist-induced currents at certain splice variants of the NMDA receptor. *Neuron* **10**, 943–954.

Ikeda, K., Nagasawa, M., Mori, H., Araki, K., Sakimura, K., Watanabe, M., Inoue, Y. & Mishina, M. (1992). Cloning and expression of the ε4 subunit of the NMDA receptor channel. *FEBS Letters* **313**, 34–38.

Ishii, T., Moriyoshi, K., Sugihara, H., Sakurada, K., Kadotani, H., Yokoi, M., Akazawa, C., Shigemoto, R., Mizuno, N., Masu, M. & Nakanishi, S. (1993). Molecular characterization of the family of the *N*-methyl-D-aspartate receptor subunits. *Journal of Biological Chemistry* **268**, 2836–2843.

Jahr, C. E. & Stevens, C. F. (1987). Glutamate activates multiple single channel conductances in hippocampal neurons. *Nature* **325**, 522–525.

Kourie, J. I., Laver, D. R., Junankar, P. R., Gage, P. W. & Dulhunty, A. F. (1996). Characteristics of two types of chloride channel in sarcoplasmic reticulum vesicles from rabbit skeletal muscle. *Biophysical Journal* **70**, 202–221.

Kutsuwada, T., Kashiwabuchi, N., Mori, H., Sakimura, K., Kushiya, E., Araki, K., Meguro, H., Masaki, H., Kumanishi, T., Arakawa, M. & Mishina, M. (1992). Molecular diversity of the NMDA receptor channel. *Nature* **358**, 36–41.

Llano, I., Marty, A., Armstrong, C. M. & Konnerth, A. (1991). Synaptic- and agonist-induced excitatory currents of Purkinje cells in rat cerebellar slices. *Journal of Physiology* **434**, 183–213.

McBain, C. J. & Mayer, M. L. (1994). *N*-methyl-D-aspartic acid receptor structure and function. *Physiological Reviews* **74**, 723–760.

Mariani, J. & Changeux, J.-P. (1981). Ontogenesis of olivocerebellar relationships. I. Studies by intracellular recordings of the multiple innervation of Purkinje cells by climbing fibers in the developing rat cerebellum. *Journal of Neuroscience* **1**, 696–702.

Mayer, M. L., Westbrook, G. L. & Guthrie, P. B. (1984). Voltage-dependent block by Mg^{2+} of NMDA responses in spinal cord neurons. *Nature* **309**, 261–263.

Meguro, H., Mori, H., Araki, K., Kushiya, E., Kutsuwada, T., Yamazaki, M., Kumanishi, T., Arakawa, M., Sakimura, K. & Mishina, M. (1992). Functional characterization of a heteromeric NMDA receptor channel expressed from cloned cDNAs. *Nature* **357**, 70–74.

Momiyama, A., Feldmeyer, D. & Cull-Candy, S. G. (1995). Single channel characteristics of NMDA receptors in Purkinje cells in thin slices of neonatal rat cerebellum. *Journal of Physiology* **483.P**, 162*P*.

Monyer, H., Sprengel, R., Schoepfer, R., Herb, A., Higuchi, M., Lomeli, H., Burnashev, N., Sakmann, B. & Seeburg, P. H. (1992). Heteromeric NMDA receptors: Molecular and functional distinction of subtypes. *Science* **256**, 1217–1221.

Monyer, H., Burnashev, N., Laurie, D. J., Sakmann, B. & Seeburg, P. H. (1994). Developmental and regional expression in the rat brain and functional properties of four NMDA receptors. *Neuron* **12**, 529–540.

Moriyoshi, K., Masu, M., Ishii, T., Shigemoto, R., Mizuno, N. & Nakanishi, S. (1991). Molecular cloning and characterization of the rat NMDA receptor. *Nature* **354**, 31–37.

Nowak, L., Bregestovski, P., Ascher, P., Herbet, A. & Prochiantz, A. (1984). Magnesium gates glutamate-activated channels in mouse central neurones. *Nature* **307**, 462–465.

Perkel, D. J., Hestrin, S., Sah, P. & Nicoll, R. A. (1990). Excitatory synaptic currents in Purkinje cells. *Proceedings of the Royal Society* B **241**, 116–121.

Petralia, R. S., Wang, Y.-X. & Wenthold, R. J. (1994). The NMDA receptor subunits NR2A and NR2B show histological and ultrastructural localization patterns similar to those of NR1. *Journal of Neuroscience* **14**, 6102–6120.

Rabacchi, S., Bailly, Y., Delhaye-Bouchaud, N. & Mariani, J. (1992). Involvement of the *N*-methyl-D-aspartate (NMDA) receptor in synapse elimination during cerebellar development. *Science* **256**, 1823–1825.

Rosenmund, C., Legendre, P. & Westbrook, G. L. (1992). Expression of NMDA channels on cerebellar Purkinje cells acutely dissociated from newborn rats. *Journal of Neurophysiology* **68**, 1901–1905.

Sheng, M., Cummings, J., Roldan, L. A., Jan, Y. N. & Jan, L. Y. (1994). Changing subunit composition of heteromeric NMDA receptors during development of rat cortex. *Nature* **368**, 144–147.

Stern, P., Béhé, P., Schoepfer, R. & Colquhoun, D. (1992). Single-channel conductances of NMDA receptors expressed from cloned cDNAs: comparison with native receptors. *Proceedings of the Royal Society* B **250**, 271–277.

Tölle, T. R., Berthele, A., Zieglgänsberger, W., Seeburg, P. H. & Wisden, W. (1993). The differential expression of 16 NMDA and non-NMDA receptor subunits in the rat spinal cord and in periaqueductal gray. *Journal of Neuroscience* **13**, 5009–5028.

Tsuzuki, K., Mochizuki, S., Iino, M., Mori, H., Mishina, M. & Ozawa, S. (1994). Ion permeation properties of the cloned mouse $\epsilon 2/\zeta 1$ NMDA receptor channel. *Molecular Brain Research* **26**, 37–46.

Wafford, K. A., Bain, C. J., Le-Bourdelles, B., Whiting, P. J. & Kemp, J. A. (1993). Preferential co-assembly of recombinant NMDA receptors composed of three different subunits. *NeuroReport* **4**, 1347–1349.

Watanabe, M., Mishina, M. & Inoue, Y. (1994*a*). Distinct spatiotemporal distribution of the *N*-methyl-D-aspartate receptor channel subunit mRNAs in the mouse cervical cord. *Journal of Comparative Neurology* **345**, 314–319.

Watanabe, M., Mishina, M. & Inoue, Y. (1994*b*). Distinct spatio-temporal expressions of five NMDA receptor channel subunit mRNAs in the cerebellum. *Journal of Comparative Neurology* **345**, 513–519.

Wyllie, D., Béhé, P., Edmonds, B., Nassar, M., Schoepfer, R. & Colquhoun, D. (1995). Whole-cell and single-channel currents from recombinant NMDA NR1/2D receptors expressed in *Xenopus* oocytes. *Journal of Physiology* **491.P**, 135*P*.

Yamazaki, M., Mori, H., Araki, K., Mori, K. J. & Mishina, M. (1992). Cloning, expression and modulation of a mouse NMDA receptor subunit. *FEBS Letters* **300**, 39–45.

Acknowledgements

This work was supported by The Wellcome Trust. S.G.C.-C.'s research programme is supported in part by an International Research Scholars Award from the Howard Hughes Medical Institute. Akiko Momiyama was funded by a Wellcome Travelling Fellowship. We would like to thank Brian Edmonds, Mark Farrant, Alasdair Gibb and Trevor Lewis for helpful discussions and valuable comments on the manuscript, and David Colquhoun for his generous help with software for single-channel analysis.

Author's present address

D. Feldmeyer: Max-Planck-Institut für medizinische Forschung, Abteilung Zellphysiologie, Jahnstrasse 29, D-69120 Heidelberg, Germany.

Authors' email addresses

S. G. Cull-Candy: s.cull-candy@ucl.ac.uk

D. Feldmeyer: feldmeyr@sunny.mpimf-heidelberg.mpg.de

A. Momiyama: a.momiyama@ucl.ac.uk

Received 18 December 1995; accepted 3 March 1996.